Anomalous Ocean Tide Loading Displacements in Western Europe Suggest Mantle Anelasticity

Peter.Clarke@newcastle.ac.uk

Peter J Clarke[1], Machiel S Bos[2], Nigel T Penna[1], Maxim Keshin[1,*], Trevor F Baker[3]

[1] School of Civil Engineering and Geosciences, Newcastle University, UK (* now at Trimble Terrasat GmbH, Munich, Germany) • [2] CIIMAR/CIMAR, University of Porto, Portugal • [3] NERC National Oceanography Centre, Liverpool, UK (retired)

1. Introduction

Ocean tide loading (OTL) is the solid Earth's response to the spatially and temporally varying bottom pressure and gravitational attraction of the ocean, which redistributes tidally at semi-diurnal, diurnal and longer periods. Around NW Europe, the M2 lunar semi-diurnal constituent (**Figure 1**) is the dominant ocean tide.

OTL causes radial and lateral displacements of Earth's surface, which may be computed by convolving the complex-valued ocean tidal height $Z(\mathbf{r}')$ with a Green's function $G(\mathbf{r}-\mathbf{r}')$ which depends on Earth's rheological properties:

$$u(\mathbf{r}) = \int_{\Omega} \rho G(\mathbf{r}-\mathbf{r}') Z(\mathbf{r}') d\Omega$$

where ρ is the density of sea water and the locations $\mathbf{r}'$ span the oceanic domain Ω. We consider radial displacement, using Green's functions initially derived from the spherically-symmetric Preliminary Reference Earth Model PREM (Dziewonski & Anderson, 1981).

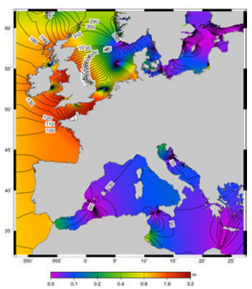

Figure 1. Amplitude and phase of the M2 tide around western Europe, according to the FES2004 model (Lyard *et al.*, 2006).

OTL displacements (OTLD) vary from a few mm to several cm in amplitude and are detectable using geometric space geodesy (*e.g.* Allinson *et al.*, 2004; Thomas *et al.*, 2007). Where ocean tides are poorly determined, geodetic measurements of OTLD may be used to validate numerical ocean tide models (*e.g.* King *et al.*, 2005); conversely, if loads are well known, loading displacements may shed light on Earth rheology (*e.g.* Ito & Simons, 2011).

2. GPS observations

Here, we estimate OTLD for the 8 major sub-daily tidal constituents, from GPS data at 200 sites spanning at least 3 years (median 1484 days) in the interval 1998-2010, using the Precise Point Positioning mode of the GIPSY/OASIS software (v5.0), with JPL reprocessed orbits and clocks, 7° elevation cut-off, body tides modelled according to the IERS 2003 conventions, and the VMF1 mapping function. We test three strategies:

(1) "Total harmonic" – essentially as Thomas *et al.* (2007): 3-d in- and out-of-phase harmonic displacements estimated in 24 h batches with no *a priori* OTLD, stacked annually, nodally corrected, then finally combined.

(2) "Residual harmonic" – similar to (1), but *a priori* OTLD computed using FES2004 and removed at the observation level from major and minor constituents (using hardisp.f), so no nodal corrections required.

(3) "Kinematic" – similar to (2), but random-walk positions estimated at 5 min intervals; amplitudes and phases later estimated via a Lomb-Scargle periodogram.

The methods yield OTLD estimates typically within 0.5 mm of each other, so we adopt (2) which is relatively insensitive to the *a priori* OTLD (**Figure 2a**). Residual OTLDs (**Figure 2b**) reach 3 mm.

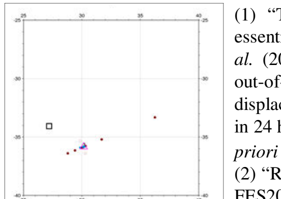

Figure 2a. Phasor plot of M2 radial OTLD at site NEWL, in mm. Black square: computed OTLD. Observed OTLD is estimated using the "residual harmonic" technique (pink triangle: best estimate; solid red circles: varying *a priori* vertical OTLD amplitude by ×0.1, ×0.5, ×2, ×5; open red circles: varying *a priori* radial OTLD phase by ±5°, ±20°; blue and green symbols similarly for *a priori* east and north OTLD).

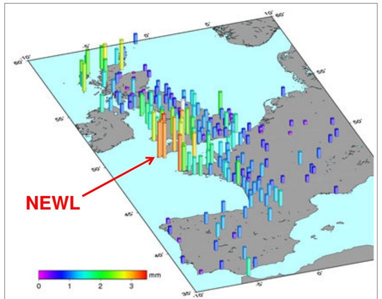

Figure 2b. Amplitudes of residual M2 radial OTLD in western Europe, using the "residual harmonic" technique (see text). The *a priori* OTLD varies in amplitude from ~2 mm in central Europe to ~44 mm at the western margins. The estimated observational uncertainty is ~0.5 mm.

3. Ocean tide, crustal, or body tidal causes?

Ocean tide models are often considered to be the largest source of error in computing OTLD, but they show good agreement in this region (**Figure 3**), limited mainly by the coarser grid size of some models. Their consistency with tide and bottom pressure gauge data is sub-dm for most areas, and sub-cm for pelagic gauges. For example, at NEWL the main contributions to OTLD come from the Celtic Sea and immediate vicinity, where discrepancies between tide models and observations barely exceed 1% and show no systematic bias. Similarly, we discount errors in the Green's function caused by local crustal structure and rheology; varying the Green's function according to the crustal models of Holder & Bott (1971) for SW England or Morgan *et al.* (2000) for NW Scotland makes less than 0.5 mm difference to computed OTLD. Finally, we discount errors in the body tide models in the IERS 2003 Conventions; although lower-mantle anelastic effects are at ~0.7 mm and may contain errors, our data show no systematic large-scale latitudinal or longitudinal variations diagnostic of this.

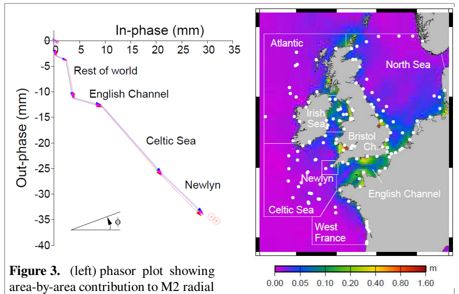

Figure 3. (left) phasor plot showing area-by-area contribution to M2 radial OTLD at NEWL, using a PREM-based Green's function and 4 recent ocean tide models; discrepancies between these are much smaller than to observed OTLD (circles/crosses). (right) rms of 5 global M2 tide models around NW Europe differenced from FES2004, showing locations of tide and bottom pressure gauges.

5. New Green's functions

We explore asthenospheric rheology in two ways. (**Figure 5a**) Least-squares estimation of a piecewise linear (in log ψ) empirical Green's function tapering to PREM for ψ<0.05° and ψ>10°, and comparison with forward models of Green's functions computed with various reductions in shear modulus μ in the PREM asthenosphere (80-220 km). (**Figure 5b**) Downhill simplex search for best-fitting values of asthenospheric depth, thickness and scaling of μ. We find that (a) a 20% drop in μ in the PREM asthenosphere, or (b) a drop of around half this over twice the depth range, both fit the data reasonably well.

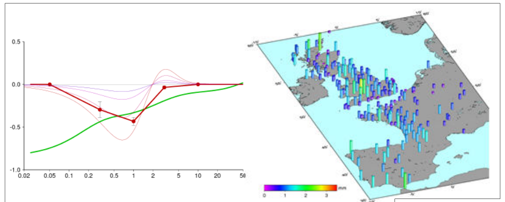

Figure 5a. (left) empirical Green's function differences (×100) from PREM (real part, thick red line) as a function of angular separation ψ, compared with those calculated for 5%, 10%, 20%, 30% reduction in asthenospheric μ (blue to red thin lines). The total PREM Green's function is shown as the thick green line. (right) magnitude of radial M2 OTLD residuals using this empirical Green's function.

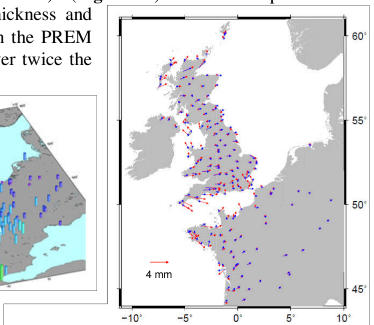

Figure 5b. Observed M2 radial OTLD residual phasors using the PREM Green's function (red) and those using an optimised Green's function which incorporates an 11% reduction in the shear modulus between depths of 50-330 km.

4. Upper mantle anelasticity?

Instead, we note the similarity between the OTLD residuals (**Figure 2b**) and those locations where significant OTLD occurs due to oceanic regions with an angular separation ψ of 0.5°-2° between the vectors **r** and **r′** (**Figure 4**). This range of ψ suggests that poorly modelled rheology within the asthenospheric depth range 25-400 km is responsible for the residual OTLD. Importantly, OTLD is the only well-constrained phenomenon sensitive to asthenospheric rheology at timescales intermediate between those of seismic waves (10^0–10^3 s) and post-seismic or glacio-isostatic adjustment (10^8–10^{12} s): body tides are mostly sensitive to the mid/lower mantle.

Frequency-dependent elasticity may be modelled (Dahlen & Tromp, 1998; Benjamin *et al.*, 2006) as shear dispersion (change in amplitude) with shear dissipation (change in phase), but no accompanying changes in the bulk modulus. Our observations show mostly amplitude discrepancies, *i.e.* dispersion is the dominant factor.

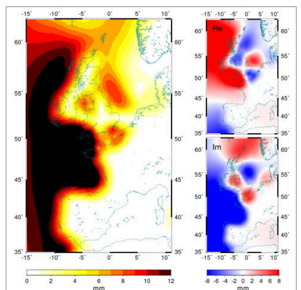

Figure 4. Radial OTLD contribution at each location from angular separations of 0.5°-2° (left, magnitude; right, real and imaginary components).

6. Conclusions

We have shown that significant discrepancies exist in western Europe between observed OTLD and that computed using PREM. Ocean tide model, crustal, and body tide causes can be discounted, whereas moderate changes in asthenospheric shear modulus, potentially due to anelastic effects, lead to a good fit with the data. OTLD is the only well-constrained phenomenon sensitive to anelasticity at this depth range and timescale.

References

Agnew, D. (1997). NLOADF: a program for computing ocean-tide loading. *J. Geophys. Res.*, **102**(B3), 9109-9110.

Allinson, C.R., P.J. Clarke, S.J. Edwards, M.A. King, T.F. Baker & P.R. Cruddace (2004). Stability of direct GPS estimates of ocean tide loading. *Geophys. Res. Lett.*, **31**(15), L15603.

Benjamin, D., J. Wahr, R. Ray, G.D. Egbert & S.D Desai (2006). Constraints on mantle anelasticity from geodetic observations, and implications for the J_2 anomaly. *Geophys. J. Int.*, **165**, 3-16.

Dahlen, F.A., & J. Tromp (1998). *Theoretical global seismology*. Princeton University Press, Princeton, NJ.

Dziewonski, A.M., & D.L. Anderson (1981). Preliminary Reference Earth Model. *Phys. Earth. Planet. Int.*, **25**, 297-356.

Holder, A.P., & M.H.P. Bott (1971). Crustal structure in the vicinity of south-west England. *Geophys. J. R. Astr. Soc.* **23**, 465-489.

Ito, T., & M. Simons (2011). Probing asthenospheric density, temperature, and elastic moduli below the western United States. *Science*, **332**, 947-951.

King, M.A., N.T. Penna, P.J. Clarke & E.C. King (2005). Validation of ocean tide models around Antarctica using onshore GPS and gravity data. *J. Geophys. Res.*, **110**(B8), B08301.

Lyard, F., F. Lefevre, T. Letellier & O. Francis (2006). Modelling the global ocean tides: modern insights from FES2004. *Ocean Dynamics*, **56**, 394-415.

Morgan, R.P.L., *et al*. (2000). Lithospheric structure north of Scotland – I: P-wave modelling. *Geophys. J. Int.* **142**, 716-736.

Thomas, I.D., M.A. King & P.J. Clarke (2007). A comparison of GPS, VLBI and model estimates of ocean tide loading displacements. *J. Geodesy*, **81**(5), 359-368.

Acknowledgements

This work was funded in the UK by NERC grant NE/C003438/1 to PJC and NTP. GPS data were obtained from the EUREF Permanent GPS Network (www.epncb.oma.be), Institut Geographique National (rgp.ign.fr) and NERC BIG F (www.bigf.ac.uk). We thank NASA JPL for the GIPSY/OASIS software, and Duncan Agnew for the routines hardisp.f (used in GIPSY) and nloadf.f (Agnew, 1997) used to compute partial sums of ocean tides.